



---

## **A New Green Salamander in the Southern Appalachians: Evolutionary History of *Aneides aeneus* and Implications for Management and Conservation with the Description of a Cryptic Microendemic Species**

Authors: Patton, Austin, Apodaca, Joseph J., Corser, Jeffrey D., Wilson, Christopher R., Williams, Lori A., et al.

Source: *Copeia*, 107(4) : 748-763

Published By: The American Society of Ichthyologists and Herpetologists

URL: <https://doi.org/10.1643/CH-18-052>

# A New Green Salamander in the Southern Appalachians: Evolutionary History of *Aneides aeneus* and Implications for Management and Conservation with the Description of a Cryptic Microendemic Species

Austin Patton<sup>1,¶</sup>, Joseph J. Apodaca<sup>2,¶</sup>, Jeffrey D. Corser<sup>3</sup>, Christopher R. Wilson<sup>4</sup>, Lori A. Williams<sup>5</sup>, Alan D. Cameron<sup>5</sup>, and David B. Wake<sup>6</sup>

**Green salamanders (Plethodontidae: *Aneides aeneus*) are rock outcrop habitat specialists, possessing numerous unique morphological adaptations (e.g., prehensile tail and squared toe-pads) for climbing. Some authors believe *A. aeneus*, which is widely distributed across the Appalachian Mountains of the inland eastern United States, comprises a species complex due to substantial karyotypic variation among populations. We conducted a population genetic and phylogenetic study across the range of *A. aeneus* and discovered substantial genetic structure, including four distinct lineages, one of which we describe as *Aneides caryaensis*, new species. Restricted to a narrow geographic distribution in western North Carolina, this species faces pressing conservation threats due to rapid real estate and tourism development in the area. We also recommend the recognition of three geographically distinct and reciprocally monophyletic lineages as evolutionarily significant units due to strong mitochondrial and nuclear differentiation among them. *Aneides aeneus* has been petitioned for listing under the Endangered Species Act, and our study further highlights the need for conservation management of this complex. Our formal recognition of the extent of genetic and evolutionary diversification of the complex is a critical step in establishing conservation strategies.**

THE global decline of amphibians as a result of rapid growth of human populations and their expansive impact on natural environments is well documented (Petranka, 1998; Collins and Storfer, 2003; Becker et al., 2007), with many species facing rapid declines and extinction (Pechmann and Wilbur, 1994; Alford and Richards, 1999; Stuart et al., 2006; Wake, 2012). A major challenge in worldwide amphibian conservation efforts is that many amphibian species are characterized by a highly conserved morphology (Cherty et al., 1978; Wake, 1991; Stuart et al., 2006; Kozak and Wiens, 2010). This morphological conservatism in turn exacerbates the challenge of delimiting species, thus preventing meaningful assessment of their true conservation status. Inaccurate or incomplete taxonomy may exacerbate population declines and elevate extinction risks through the lack of necessary conservation interventions.

Species delimitation is one of the most difficult and controversial subfields of ecology and evolutionary biology (De Queiroz, 2007; Wiens, 2007), yet given trends in defaunation (Dirzo et al., 2014), the need for characterizing extant diversity is growing. Modern molecular tools, a more unified species concept (i.e., the generalized lineage concept; De Queiroz, 2007), and tree-based delimitation methods have led to the identification of a plethora of unique taxa from cryptic complexes, establishing them as invaluable tools in this endeavor (Bogart and Tandy, 1976; Hillis et al., 1983; Highton et al., 1989; Wynn and Heyer, 2001; Jockusch and Wake, 2002; Pauly et al., 2006; Elmer et al., 2013).

A common approach to facilitate species delimitation is to leverage phylogenetic species delimitation methods (e.g., Roy et al., 2014; Kotsakiozi et al., 2018; Titus et al., 2018). Based on, in part, the phylogenetic species concept, these

methods use phylogenetic and coalescent models to guide the delimitation of species from empirical phylogenies (e.g., Pons et al., 2006; Yang and Rannala, 2010; Zhang et al., 2013; Yang, 2015). However, methods leveraging the multispecies coalescent have recently been demonstrated to often delimit population structure, not species (Sukumaran and Knowles, 2017). To avoid this concern, at least in part, methods reliant on models other than the multispecies coalescent may be used (e.g., Poisson Tree Processes [PTP; Zhang et al., 2013]). Species delimitation necessitates the use of multiple lines of evidence (e.g., molecular, morphological, ecological, and biogeographical). Although no single phylogenetic species delimitation method is invulnerable to the concerns voiced by Sukumaran and Knowles (2017), these approaches serve as a valuable complement to other sources of evidence when describing cryptic diversity.

Cryptic salamander complexes frequently occur in areas that contain a rich variety of climatic zones, geologic formations, and habitat diversity (e.g., California Floristic Province [Myers et al., 2000; Lapointe and Rissler, 2005; Rissler et al., 2006; Rissler and Apodaca, 2007; Reilly and Wake, 2015] and eastern and southern Mexican highlands [Rovito et al., 2013]). The Appalachian Mountains of the eastern United States display many of these attributes and are one of the oldest continuously exposed land masses on earth. They have a rich geologic history (Pickering et al., 2003), a diverse set of climatic regions, and a multitude of rare ecosystem types, many of which are globally threatened (Noss et al., 1995). The southern Appalachians are especially rich in biodiversity and endemism (Pickering et al., 2003) and are a center of diversity for many taxa.

<sup>1</sup> School of Biological Sciences, Washington State University, Pullman, Washington 99164.

<sup>2</sup> Amphibian and Reptile Conservancy and Tangled Bank Conservation, 128 Bingham Road, Suite 1150, Asheville, North Carolina 28806; Email: JJ@tbconservation.org. Send reprint requests to this address.

<sup>3</sup> New York Natural Heritage Program, SUNY College of Environmental Science and Forestry, 625 Broadway, 5<sup>th</sup> Floor, Albany, New York 12233.

<sup>4</sup> Conservation Ecology LLC, 6 Penny Ct., Hendersonville, North Carolina 28739.

<sup>5</sup> North Carolina Wildlife Resources Commission, 177 Mountain Laurel Lane, Fletcher, North Carolina 28732.

<sup>6</sup> Museum of Vertebrate Zoology, University of California, Berkeley, California 94720-3160.

¶ These authors contributed equally to this work.

Submitted: 20 April 2018. Accepted: 4 October 2019. Associate Editor: B. Stuart.

© 2019 by the American Society of Ichthyologists and Herpetologists DOI: 10.1643/CH-18-052 Published online: 3 December 2019

Notably, salamanders of the family Plethodontidae are extremely diverse in this region and have high levels of both endemism and cryptic diversity (Camp and Wooten, 2016). A classic example of non-adaptive radiation (Rundell and Price, 2009), salamanders of the genus *Plethodon* diversified rapidly in the eastern United States, yet are extremely morphologically conserved (Kozak et al., 2006). Hypothesized to be driven by phylogenetic niche conservatism (Kozak and Wiens, 2006), this radiation has produced multiple cryptic species that have been delimited, at least in part, using molecular data (e.g., Highton, 1995, 1999; Highton and Peabody, 2000; Kuchta et al., 2018).

The identification of cryptic species is especially important for species that are experiencing rapid population decline. One such susceptible species is the green salamander (*Aneides aeneus*), which is listed as Near-threatened with decreasing populations by the IUCN Red List (Hammerson, 2004), Vulnerable by NatureServe (Hammerson and Dirrigr, 2017), and has been petitioned for listing under the federal Endangered Species Act. Note, however, that both the IUCN and NatureServe threat categories are in need of revision, having last been assessed 14 and 11 years ago, respectively. Consequently, these threat categories likely do not reflect the present-day population trends.

*Aneides aeneus* is a habitat and microhabitat specialist, making the species particularly vulnerable to habitat loss and fragmentation. These salamanders are generally associated with crevices and hollows of rock outcrop, woody, and arboreal habitats within cove forests (Gordon, 1952; Cupp, 1991; Waldron and Humphries, 2005; Smith et al., 2017). These scansorial animals are frequently found in shady crevices in rock outcrops in mixed mesophytic forests from ~300 to 1200 m elevation. Although they have been observed to exhibit arboreal tendencies, they typically are restricted to areas harboring rock outcrops (Gordon, 1952; Waldron and Humphries, 2005; Smith et al., 2017). A large number of nesting sites have been detected on rock faces (but see Pope, 1928), which may in turn lead breeding populations to be patchily distributed (Petranka, 1998; Corser, 2001). In the 1970s, green salamander populations collapsed in the disjunct Blue Ridge Escarpment (Snyder, 1983, 1991; Corser, 2001). However, those outside of the escarpment within the western portion of their range remained stable (Snyder, 1991). Corser (2001) studied trends in several populations in the Blue Ridge Escarpment throughout the 1990s and found a 98% decline in relative abundance since 1970; extensive surveys over the last 30 years by the North Carolina Wildlife Resources Commission (NCWRC) indicate that declines appear to have continued in these populations over the last decade and a half.

In this study, we examined spatial genetic patterns in *A. aeneus* through the integration of population genetic and phylogenetic methods. We analyzed 12 polymorphic microsatellite loci from specimens collected from across the range of *A. aeneus* in western North Carolina, including samples obtained from Virginia to represent the northern Appalachian portion of their range. In doing so, we sought to define geographic patterns of genetic variation and population structuring across the range of *A. aeneus* in western North Carolina. We additionally conducted phylogenetic analyses using 1) targeted mitochondrial sequences (Cyt *b* and 12S rDNA) of 74 samples across the range of *A. aeneus* and 2) a nuclear multilocus SNP dataset for ten individuals across the range obtained using 3RAD-seq (Bayona-Vásquez et al., 2019; bioRxiv:205799). Population assignments obtained using

microsatellites are concordant with the identification of clades in the phylogenetic component of this study. Preliminary morphological comparisons among near-topotypic *A. aeneus* and the clade restricted to the Hickory Nut Gorge (HNG) of western North Carolina reveals cryptic, but unequivocal differentiation that is concordant with molecular evidence. As such, we describe this lineage as *Aneides caryaensis*, a new species, the first cryptic species to be described within the subgenus *Castaneides* (eastern *Aneides*: Dubois and Raffaëlli, 2012).

## MATERIALS AND METHODS

**Population sampling.**—For the microsatellite analysis, we collected tail tips (<5 mm) from each specimen and immediately preserved them in 95% ethanol. We then stored these in a –70°C freezer at Tangled Bank Conservation until extraction. We sampled in the Blue Ridge Escarpment (BRE: 197 samples) and Hickory Nut Gorge (HNG: 28 samples) areas of western North Carolina. An additional 17 samples collected from western Virginia were donated to the study by the University of Virginia's College at Wise and were stored in a like manner. In total, 242 samples were collected for microsatellite analysis.

For analysis of mtDNA, we employed an iterative strategy of geographically dispersed sampling, analysis, targeted re-sampling, and re-analysis (e.g., Jockusch and Wake, 2002; Morando et al., 2003; Moritz et al., 2009). From the late 1990s to the middle 2000s, we collected tail clippings from specimens at 72 different populations (74 total samples) and immediately placed them in 95% ethanol and maintained them at –80°C until extraction.

**Microsatellite discovery.**—Total genomic DNA was extracted from eight individuals using Qiagen DNeasy kits (Qiagen, Valencia, CA) according to the manufacturer's protocols. An Illumina paired-end shotgun library was then prepared and sequenced on an Illumina HiSeq. Resulting reads were analyzed using the program PAL Finder v0.02.03 (Castoe et al., 2012). This program extracted reads containing di-, tri-, tetra-, penta-, and hexanucleotide microsatellite repeats. Resultant positive reads were then analyzed with Primer3 (version 2.0.0; Koressaar and Remm, 2007; Untergasser et al., 2012) to design primer sequences. Only those loci with sequences that were identified once or twice in our total set of reads were selected for optimization in order to avoid primer sequences that may amplify in multiple locations across the genome.

**Primer testing and validation.**—From the set of putative microsatellite loci described above, we selected 48 loci for amplification and polymorphism across 20 individuals from three populations according to the protocol described by Eschbach and Schöning (2013). This protocol does not necessitate individual genotypes. Instead, presence/absence of alleles in pooled DNA samples are used to estimate within and among population variability in allele frequency. Loci were then scored according to the degree of this variation using the scoring procedure described by Eschbach and Schöning (2013).

Multiplex PCR reactions were conducted using Qiagen Multiplex PCR kits (Qiagen, Valencia, CA) in accordance to the manufacturer's protocols, albeit conducted in 10 µL volume reactions. Each locus was amplified individually using labeled primers. PCR cycles consisted of an initial 15

**Table 1.** Results of the analysis of molecular variance (AMOVA).

Source of variation	Percent variance	P-value
Within population	0.712	
Among population	0.288	0.001

min denaturing step at 95°C, followed by 35 cycles of 30 sec denaturing at 94°C, 90 sec annealing step at 57°C, and a 60 sec extension at 72°C. A 30 min extension step at 60°C followed the 35 cycles, prior to cooling the product to 4°C. Resultant amplification products were then sized on a ABI 3730 DNA Analyzer at Florida State University using a GS500HDROX size standard. Results were then scored using Geneious version 6.1.6 (Kearse et al., 2012). Of the 48 loci screened, 12 were sufficiently polymorphic within and among populations and amplified consistently with easily scored genotypes (Table 1).

**Microsatellite characterization.**—With the 12 polymorphic microsatellite loci identified using the method of Eschbach and Schöning (2013), we then validated these loci by genotyping the 242 samples collected for this study. Procedures for amplification, genotyping, and scoring of these samples was the same as previously described. Once scored, observed ( $H_O$ ) and expected ( $H_E$ ) heterozygosities and number of alleles per locus ( $k$ ) were calculated using GenoDive v2.0b25 (Meirmans and van Tienderen, 2004). The presence and frequency of null alleles at each locus were tested for using the R package Genepop (Rousset, 2008).

**Microsatellite analysis.**—To identify how populations are structured on the basis of geospatial patterns of genetic variation, we used TESS 2.3.1 (Chen et al., 2007). TESS is a program that is applied in a Bayesian framework, building Voronoi tessellations to group individuals through the identification of geographical discontinuities in allele frequencies, assuming that geographically clustered individuals will be more likely to have similar allele frequencies than more distant individuals. The number of populations ( $K$ ) was estimated by running five repeat models for  $K = 2$  through  $K = 6$ , in which 1,000,000 iterations with a burn-in of 1,000 were conducted. As suggested by François and Durand (2010), Deviance Information Criterion (DIC: Spiegelhalter et al., 2002) values were averaged between repeat runs, plotted against their respective  $K$ s, and the value of  $K$  at which DIC plateaued was chosen as our best supported model. Populations that were defined according to this approach were then used in later phylogenetic analyses.

Once populations were defined using TESS, measures of population genetic diversity were calculated in GenoDive v2.0b25 (Meirmans and van Tienderen, 2004). Specifically, we calculated Nei's inbreeding statistic,  $G_{IS}$  (Nei, 1987), to quantify within-population genetic diversity. To quantify among-population diversity, we took two approaches. We performed a locus-by-locus analysis of molecular variance (Excoffier and Laval, 2005) using 10,000 permutations and a ploidy-independent mutation model. We then calculated pairwise values of  $F_{ST}$  using 1,000 permutations for significance, followed by a Bonferroni correction. These measures served to complement our phylogenetic reconstructions, providing an indication of the extent of gene flow occurring between recovered clades.

**Targeted sequencing, alignment, and model selection.**—Genomic DNA was extracted from frozen tissues using a Puregene™ 68 kit (Gentra Systems, Inc.). Mitochondrial Cytochrome *b* (Cyt *b*) was amplified by PCR using the Cytochrome *b* primers MVZ 15 (5'-GAACTAATGGCCCA CACWWTACG-3') and Cyt b2 (5'-CCCCTCAGAATGA TATTTGTCCTA-3'; modified from Moritz et al., 1992). 12S ribosomal DNA was amplified using primers 12SJ-L (5'-AAAGRTTGGTCCTRRSCTT-3') and 12SK-H (5'-TCCRGTAIRCTTACCDTGTACGA-3') as described by Goebel et al. (1999). Amplifications began with 4 min at 94°C followed by 45 cycles at 94°C for 1 min, 50–55°C for 1 min, 72°C for 1 min, followed by 72°C for 5 min. PCR products were purified using the GeneClean II kit (Bio 101). These products were then sequenced in both directions using a 377 ABI automated sequencer and the ABI BigDye™ Terminator v3.0 Ready-Reaction Cycle Sequencing kit, but with one quarter the recommended reaction volume. Mitochondrial DNA sequences were aligned using Clustal X (Thompson et al., 1997).

Using the concatenated aligned mitochondrial sequences, we then evaluated models of nucleotide substitution using jModeltest 2.1.10 (Darriba et al., 2012). Model selection was carried out using the Bayesian information criterion (BIC: Schwarz, 1978) to evaluate the relative model fits of 88 models of evolution. A single model of nucleotide substitution was assumed for the two genes as the mitochondrion is a single non-recombining locus. Considered models included those with equal or unequal base frequencies, those that included rate variation among sites (Number Rate Categories = 6), and those with or without a proportion of invariant sites. The base tree for fitting models of nucleotide substitution was generated via Maximum Likelihood, using Subtree Pruning and Regrafting as the tree topology search operator. Cyt *b* and 12s rDNA sequences from GenBank of *A. hardii* (NC\_006338) and *A. flavipunctatus* (NC\_006327) were used as outgroups (Mueller et al., 2004).

**3RAD sequencing and bioinformatics.**—Individual extractions were normalized and prepared using a 3RAD library procedure (Adapterama III; Bayona-Vásquez et al., 2019; bioRxiv: 205799). The three enzymes used during the digestion step were BAMHI, MSPI, and ClaI. Each sample was then quadruple-indexed, limited-cycled in PCR, and cleaned using speed beads (Rohland and Reich, 2012) following the 3RAD procedure. Finally, samples were pooled together, size selected for 500 bp on a Pippin Prep (Sage Science), and sequenced on an Illumina HiSeq with a PE 150 kit (Illumina Inc.) with 5 million reads per sample. The 3RAD sequence data was demultiplexed, quality assessed, clustered, consensus called, and assembled de novo, using ipyrad v0.7.28 (Eaton and Overcast, 2016). The params file used for ipyrad is included in the supplement (see Data Accessibility).

Sequencing was done using the Illumina HiSeq 2500 platform at the University of Georgia Genomics and Bioinformatics Core. The resultant 30,524 SNPs were then filtered in VCftools v0.1.14 (Danecek et al., 2011). Resultant SNPs following our filtering met the following requirements: minimum and maximum number of alleles per site of 2, minimum mean depth of coverage of 5, minor allele frequency of 0.2 (to remove singletons), present in at least 50% of samples. Indels were removed. Using these resultant SNPs, we produced a second SNP dataset by excluding heterozygous sites.

We produced multiple sequence alignments of these concatenated filtered SNPs in fasta format using PGDspider v2.1.1.2 (Lischer and Excoffier, 2011) and custom scripts. When converting from variant call to fasta format, PGDspider produces two concatenated sequences per sample: one generated from the concatenation of the first allele across all sites, and one from the second allele across all sites. In this way, we produced two alignments—one from the first allele at each site using the homozygous only SNPs, and one produced by concatenating the haploid, concatenated sequences of the first and second allele (using all sites) as described by Margres et al. (2018).

**Mitochondrial phylogenetic reconstruction.**—To infer our phylogeny using both our Cyt *b* and 12S rDNA mitochondrial sequences using BEAST 2 (Bouckaert et al., 2014), we left clock-model, site-model, and trees linked across genes as they are inherited as a single non-recombinant locus. Parameters regarding the site model (gamma shape, substitution rate, etc.) for each gene were specified according to the best-supported model from jModeltest 2; note, however, that we allowed for six gamma rate categories as the default of four may lead to excessive discretization of rate heterogeneity (Jia et al., 2014). We used a strict-clock model as our clock prior, provided the well-documented clock-like pattern of evolution of the mitochondrial genome. Provided the 0.8% pairwise sequence divergence per million years between salamandrid genera *Taricha* and *Notophthalmus* (Tan and Wake, 1995), we used a clock rate of 0.004 substitutions/site/MY [ $(\frac{0.8\%}{2}) \div 100 = 0.004$ ]. Division by two is necessary to convert the pairwise sequence divergence to an estimate of per-branch divergence. A Yule model with a birth rate prior of 1/X was chosen to serve as an uninformative prior (Drummond and Bouckaert, 2015). All other priors were used in their default settings. The MCMC was allowed to run for 100,000,000 generations, with a burn-in of 10,000 generations, sampling every 10,000 generations.

Resulting trace files were visualized in Tracer v1.6 (Rambaut et al., 2014) to estimate Effective Sample Sizes (ESS) and to check for convergence of the chain. Trees were then uploaded into TreeAnnotator v2.3.1. A burn-in of 10% was set for the annotation, with the target tree set as the maximum clade-credibility tree. Node heights of the resultant phylogenetic tree were set using the mean heights across the posterior distribution of trees. Annotated trees were then visualized using FigTree v1.4.2 (Rambaut et al., 2014).

**Nuclear phylogenetic reconstruction.**—SNPs obtained via 3RAD-seq were then used to produce two unrooted phylogenies, one using SVDquartets (Chifman and Kubatko, 2014) in PAUP\* v4.0a157 (Swofford, 2003) as in Margres et al. (2018), and one using RAxML v8 (Stamatakis, 2014) on the CIPRES portal (Miller et al., 2010). SVDquartets uses SNPs to infer relationships among quartets of taxa under a coalescent model in which each site is assumed to have its own genealogy. Thus, the choice of concatenating each allele is compatible with this model. As input for SVDquartets, we used the concatenation of all alleles as input. In contrast, the concatenated sequence of the first allele at every homozygous site was used for RAxML.

Using SVDquartets, all quartets were estimated under the multispecies coalescent model (expecting matrix-rank 10), and these quartets were assembled using the QFM algorithm. Confidence in tree topology was quantified through non-parametric bootstrapping. A consensus tree was produced by

summarizing across bootstrapped trees using the SumTrees program as implemented in DendroPy v4.3.0 (Sukumaran and Holder, 2010) using `-force-unrooted` and `-min-clade-freq = 0.25`. Consensus trees were visualized using FigTree v1.4.3 (Rambaut et al., 2014).

Using RAxML, phylogenies were inferred under the GTR model disabling rate heterogeneity, assuming each SNP evolves independently. Bootstrapping (100 replicates) was conducted using a rapid bootstrap analysis following a search for the best scoring ML tree (`-f a` option). The best tree and bootstrap nodal support values were visualized in FigTree v1.4.3 (Rambaut et al., 2014). We implemented the Felsenstein acquisition bias for invariant sites by specifying the number of sequenced sites not included in our final set of SNPs (Leaché et al., 2015). Because the exclusion of heterozygous sites led to the removal of a large number of sites informative to distinguishing individuals from the Hickory Nut Gorge, we also inferred a phylogeny without an ascertainment bias, thus including heterozygous sites. These results may be found in the supplement (see Data Accessibility).

**Morphological materials collection.**—Specimens used for this study included seven adults (3 males, 4 females) from the Hickory Nut Gorge (see below) and a series of nine adults of *Aneides aeneus* (6 males, 3 females) in the Museum of Vertebrate Zoology (MVZ) collected from SE Fort Payne along Little River Canyon, De Kalb County, Alabama (34.39°N, 85.62°W). Herein, we explicitly tested the hypothesis that specimens from the Hickory Nut Gorge differ from topotypic *A. aeneus*.

The following measurements were used for preliminary morphological comparison: snout to posterior angle of vent (standard length, SL), head width (HW), snout to gular fold (SG), head depth at posterior angle of jaw (HD), eyelid length (EL), eyelid width (EW), anterior rim of orbit to tip of snout (ES), horizontal eye diameter (ED), anterior rim of orbit to external naris (EN), interorbital distance between angle of eyes (intercanthal distance, IC), interorbital distance between eyelids (IO), snout to forelimb (SF), distance separating external nares (internarial distance, IN), snout projection beyond mandible (SP), shoulder width (SW), distance between axilla across dorsum, snout to anterior angle of vent (SAV), axilla–groin distance (AX), number of costal interspaces overlapped by adpressed limbs (negative when overlapped, positive when not overlapped [limb interval, LI]), forelimb length (FLL), hind limb length (HLL), hand width (HAW), foot width (FW), length of third (longest) toe (T3), and length of fifth toe (T5). Measurements were made using digital calipers. Tooth counts are based on direct counts of clearly ankylosed teeth. Institutional abbreviations follow Sabaj (2016). Color information was derived from photographs of living specimens.

**Preliminary morphological comparative analyses.**—Measurements of all 18 traits were compared among topotypic *A. aeneus* and samples from the Hickory Nut Gorge using a two-tailed Welch two-sample t-test in R version 3.4.2 (R Core Team, 2017). We omitted tail measurements from animals with regenerated tails for statistical comparisons. Additionally, to test the hypothesis that the two species are distinguishable on the basis of morphology, we leveraged both Principal Components Analysis (PCA) and Linear Discriminant Analysis (LDA). For these analyses, we excluded tail measurements, as well as counts of pre-maxillary and

maxillary teeth due to the presence of missing data. We also removed costal groove counts as this character was near invariable (excluding one sample from the Hickory Nut Gorge) and thus uninformative. The remaining 14 characters were visually inspected for normality and, where necessary and possible, transformed to improve normality. Longest toe and 5<sup>th</sup> toe were log-transformed, and adpressed limbs were converted to absolute value (all values were negative) and subsequently log-transformed. Due to our low sample size, LDA was performed as follows. First, 11 of 16 samples (approximately two-thirds) were used for training, whereas the remaining five samples were to assess prediction accuracy. We then repeated this process 10,000 times, thus producing a distribution of prediction accuracies that we subsequently used to produce an estimate of mean prediction accuracy. Due to the low sample size in these analyses, we emphasize that results are preliminary in nature.

**Phylogenetic species delimitation.**—We chose to supplement our phylogenetic and population genetic analyses with species delimitation using Poisson tree processes (Zhang et al., 2013). The method Poisson tree processes (PTP) is not built around the multispecies coalescent, instead modeling the speciation process as a function of the substitution process. Briefly, PTP attempts to delimit the boundaries at which the substitution process transitions between the inter- and intraspecific substitution process as a function of the branching process, namely branch lengths. Notably, this method does not necessitate time-calibrated phylogenies, thus allowing us to use it with both of our molecular phylogenies. Further, the PTP has recently been demonstrated to perform with similar accuracy as both the Generalized Mixed Yule Coalescent (GMYC) and Bayesian Phylogenetics and Phylogeography (BPandP) and is more conservative than the GMYC (Luo et al., 2018).

We applied the PTP to both our mitochondrial and nuclear phylogenies on the PTP web server (<https://species.h-its.org/>). For each phylogeny, the analysis was run for a total of 500,000 generations, sampling every 500 generations for a total of 1,000 from the posterior. The first 10% of samples were discarded as burn-in. For the mitochondrial dataset, outgroups were retained as a reference for interspecific branching processes and to minimize false positives.

## RESULTS

**Microsatellite characterization.**—We identified, validated, and optimized 12 microsatellite loci for use in conservation studies of subgenus *Castaneides* and other members of the genus for which microsatellites have not been developed. We found these loci to possess varying levels of diversity (Table S1; see Data Accessibility). Although the prevalence of null alleles (>10%) is not trivial (Table S1; see Data Accessibility), their presence is distributed across populations (Table S2; see Data Accessibility). However, we do not believe this to be of great concern, as null alleles have only been found to inflate, not generate, population structure or impact hypothesis testing (Chapuis and Estoup, 2007; Carlsson, 2008). Thus, the presence of null alleles in our dataset is unlikely to generate the patterns of population differentiation documented herein.

**Population structuring and differentiation.**—Our analysis of population structuring in TESS (Chen et al., 2007) found that  $K = 4$  was the best-supported model according to the method

**Table 2.** Pairwise  $F_{ST}$  values for populations of *Aneides aeneus* (*Castaneides*) identified in this study. All values are statistically significant at the <0.001 level.

	BRE-1	BRE-2	HNG
BRE-2	0.076	—	—
HNG	0.289	0.305	—
VA	0.139	0.192	0.282

of François and Durand (2010; Fig. S1; see Data Accessibility). From here on, these populations will be referred to as the Blue Ridge Escarpment (BRE) populations, Hickory Nut Gorge (HNG) population, and Virginia (VA) population. Of the samples, 197 were assigned to the two populations comprising the BRE, 28 were assigned to the HNG, and 17 were assigned to the VA population (Fig. 1). Interestingly, whereas  $K$  of 3 reveals unambiguous assignment of all individuals collected from the BRE to one population, the best fit model ( $K = 4$ ) reveals apparent population structure within the BRE (Fig. 1). However, among these two populations there is appreciable admixture. Although we discovered population structuring within the BRE, individuals from VA and the HNG were always unambiguously assigned to their own populations (Fig. 1).

Results of both AMOVA (Table 1) and pairwise  $F_{ST}$  (Table 2) further revealed the extent of differentiation among populations identified by TESS. Analysis of molecular variance showed that whereas 71% of variance could be explained within populations, the remaining 29% could be explained by among-population differences ( $P = 0.001$ ). Pairwise  $F_{ST}$  revealed that whereas the two BRE populations are little differentiated ( $F_{ST} = 0.076$ ), the HNG population is highly differentiated from both BRE subpopulations (BRE-1: 0.289, BRE-2: 0.305) despite their close geographic proximity. Likewise, the HNG and VA populations are highly differentiated ( $F_{ST} = 0.282$ ). Lastly, the VA population exhibits an intermediate degree of differentiation from the two BRE subpopulations (BRE-1: 0.139, BRE-2: 0.192). Importantly, all comparisons are highly significant ( $P = 0.001$ ).

Calculations of the inbreeding coefficient (Table 3),  $G_{IS}$ , ranged greatly between populations. Notably, the first BRE population appears to be harboring an excess of heterozygosity ( $G_{IS} = -0.05$ ,  $P = 0.001$ ). In contrast, the second BRE subpopulation ( $G_{IS} = 0.103$ ,  $P = 0.001$ ) and HNG population ( $G_{IS} = 0.250$ ,  $P = 0.001$ ) are quite inbred, with the HNG faring particularly poorly. The VA population does not appear inbred ( $G_{IS} = 0.035$ ,  $P = 0.191$ ).

**Mitochondrial sequence data and model selection.**—Sequencing of mitochondrial loci Cytochrome *b* and 12S rDNA yielded aligned sequence lengths of 433 and 415 nucleotides, respectively. For our concatenated alignment, we found that TrN+G was the best supported model according to BIC as

**Table 3.** Genetic diversity and inbreeding coefficient,  $G_{IS}$ , at each population in this study.  $H_O$  is the observed heterozygosity and  $H_E$  is the expected heterozygosity within populations. Parenthetical values are the corresponding  $P$ -values for estimates of  $G_{IS}$ .

Population	$H_O$	$H_E$	$G_{IS}$
BRE-1	0.726	0.692	-0.050 (0.001)
BRE-2	0.595	0.663	0.103 (0.001)
HNG	0.455	0.607	0.250 (0.001)
VA	0.711	0.736	0.035 (0.191)

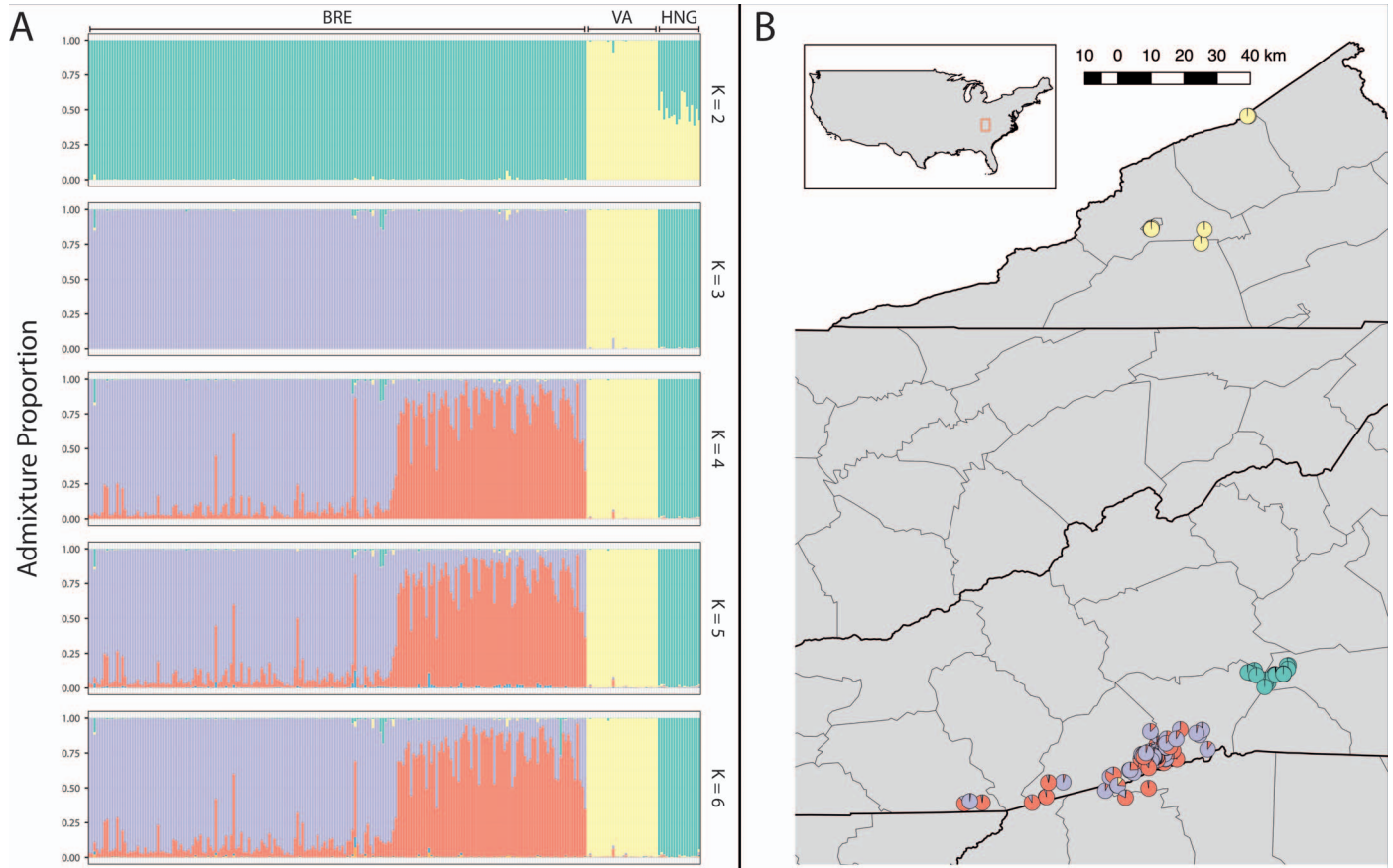


**Fig. 1.** Population structuring in *Aneides aeneus* (*Castaneides*) as identified using 12 microsatellite loci and TESS. (A) Results of running TESS assuming the number of populations ( $K$ ) ranges from two through six. Each column represents an individual, and the colors in each bar indicate the population each individual is assigned to. The height and color of each bar represents the admixture proportion for that individual. Results for a single run are shown. (B) Representation of best-fit ( $K = 4$ ) TESS results in geographic space. Samples are shown as pie charts, with colors corresponding to the populations identified in A, and the fractions corresponding to each sample's admixture proportions.

implemented in jModeltest 2. Model parameter estimates (Gamma = 0.2960, ncat = 6, Rate AC = 1, Rate AG = 4.9971, Rate AT = 1, Rate CG = 1, Rate CT = 8.9766, and Rate GT = 1.0) were thus implemented as our site model.

**Phylogenetic inference.**—Our Bayesian phylogenetic reconstruction using concatenated Cyt *b* mtDNA and 12S rDNA sequence data recovered four well-supported, reciprocally monophyletic lineages within *A. aeneus* (Fig. 2). Provided our strict molecular clock rate is accurate, the node heights (coalescent times) may be interpretable in terms of millions of years. Our tree thus indicates that the tMRCA (time to most recent common ancestor) between *A. aeneus* and our outgroups is roughly 30 MYA. The Hickory Nut Gorge lineage was inferred to be sister to all other lineages within the *A. aeneus* complex, with their tMRCA being estimated at around 11 MYA. The southern Appalachian lineage last shared a common ancestor with the lineage comprising the BRE and northern Appalachian lineages approximately 9 MYA. Lastly, the BRE and northern Appalachian lineages last shared a common ancestor around 5 MYA. Our estimates of divergence times are concordant with those of Shen et al. (2016: between 27.2 and 32.3 MYA), who used several methods to estimate the divergence times between *A. aeneus* and *A. hardii*.

Following SNP calling in iPyrad, a total of 30,524 SNPs were obtained. Filtering in VCFtools yielded final SNP dataset containing 3,550 SNPs across the ten samples. Reduction of

these sites to only those homozygous genotypes for ascertainment bias correction reduced the number of SNPs to 2,634 in RAxML.

Using SVDquartets, four well-supported groups were identified (>95% BS support: Fig. 3A) that roughly corresponded to the four clades identified in the mitochondrial phylogeny (BRE, northern Appalachians, southern Appalachians, HNG). These findings are further substantiated by our nuclear phylogeny estimated by RAxML (Fig. 3B). This phylogeny recovered three well-supported groups (BRE, southern Appalachians, and HNG), with the northern Appalachians forming a single monophyletic group despite lower support values. Notably, the HNG and southern Appalachian lineages are separated by long branches, indicating substantial genetic divergence of each clade from the rest of the *A. aeneus* species complex. Removal of heterozygous sites led to the inference of zero-value branch lengths among samples from the HNG, a fact that reiterated the low genetic diversity harbored within this population.

**Species delimitation.**—We applied the PTP to the phylogenies obtained using BEAST and RAxML. Using the mitochondrial phylogeny, the PTP identified four species with a posterior support greater than 50% (Fig. 2): southern Appalachians (59%), BRE (91%), northern Appalachians (71%), and the HNG (93%). In contrast, when applying the PTP to the nuclear tree produced by RAxML (Fig. 3), we identified three species; however, support values were low overall, likely

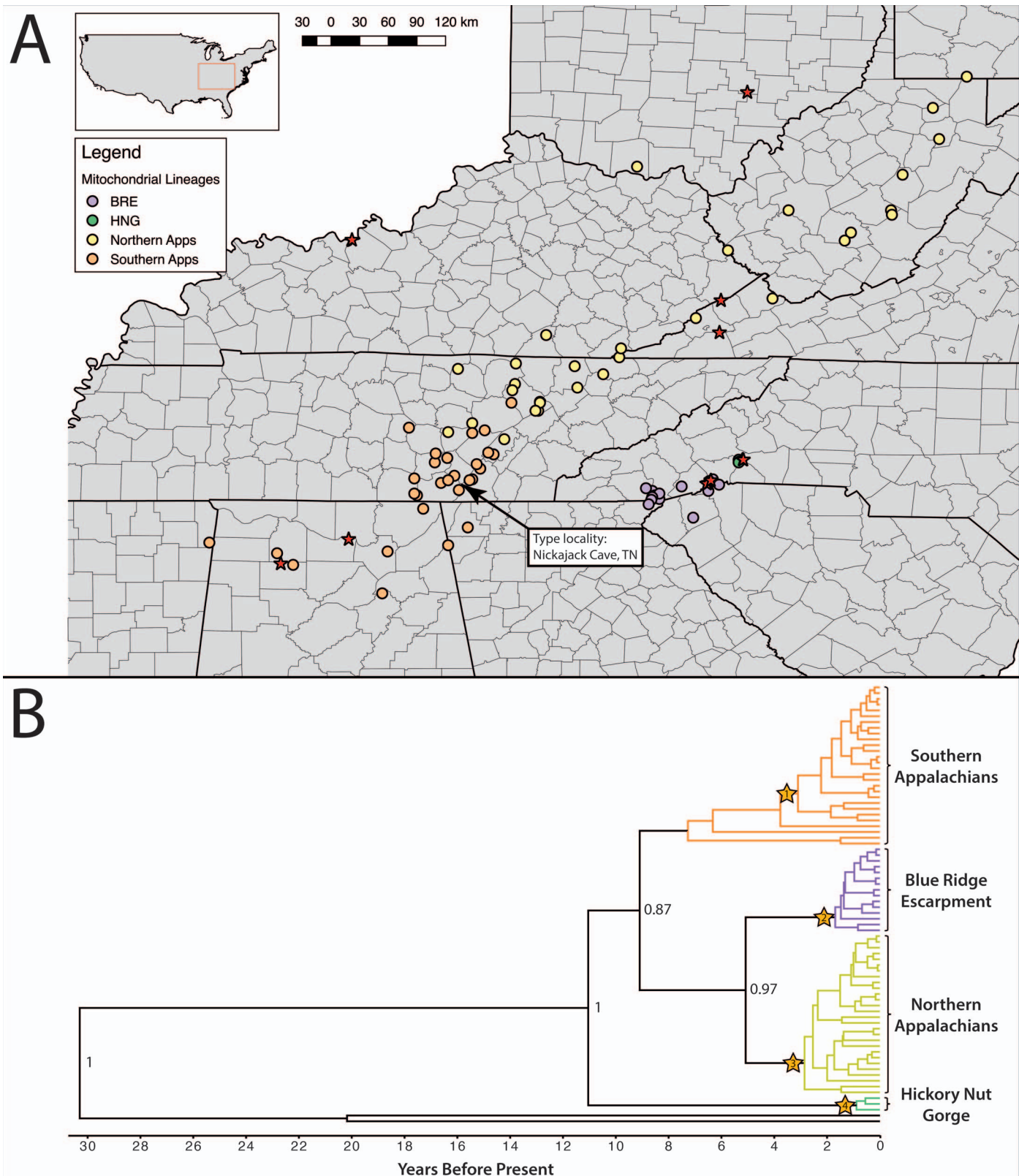


**Fig. 2.** Mitochondrial phylogenetic lineages within *Aneides aeneus* (*Castaneides*). (A) Localities of samples used in the mitochondrial phylogenetic analysis. The type locality (Nickajack Cave) is in Tennessee, at the border with Alabama; specimens from this vicinity are nested in the southern Appalachian clade. Red stars are locations used in the nuclear phylogenetic reconstruction. (B) Bayesian consensus tree of Cytochrome *b* and 12S rDNA sequences as produced by BEAST 2. Node labels represent posterior probabilities for the four main lineage splits within *A. aeneus* (*Castaneides*). Outgroup contains one voucher specimen each of *A. hardii* and *A. flavipunctatus*, obtained from GenBank. Numbered stars indicate clades identified by PTP to comprise unique species across the majority of the posterior distribution. Support values for clades are as follows: 1) 59%, 2) 91%, 3) 71%, 4) 93%. See Data Accessibility for tree file.



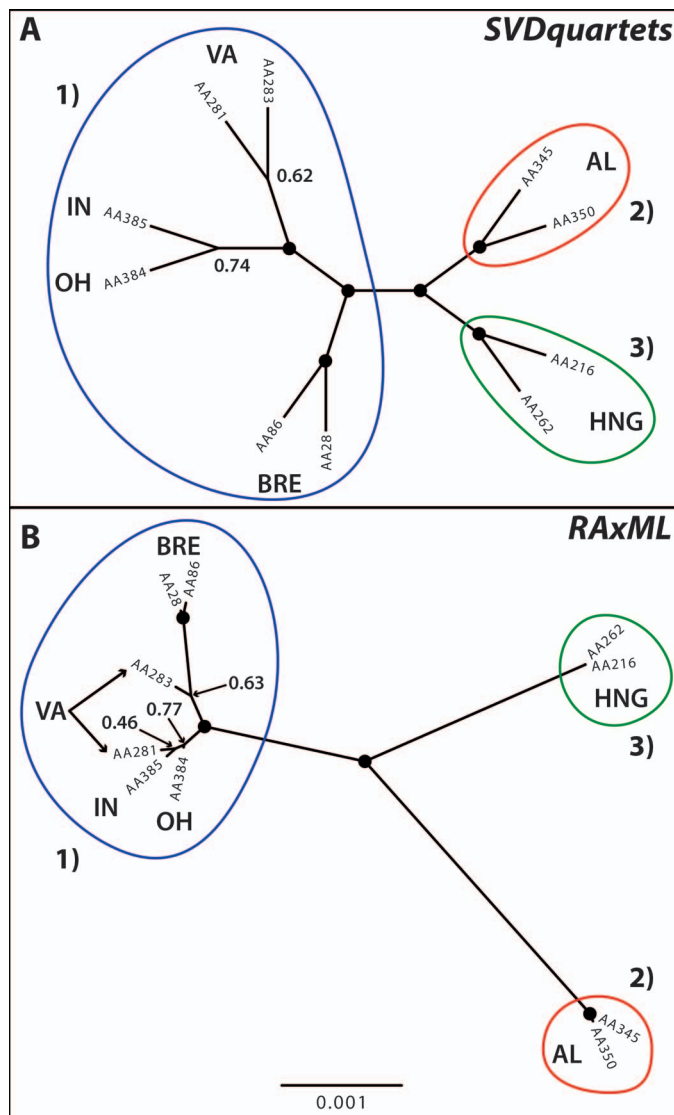


**Fig. 3.** Nuclear phylogenies as estimated by (A) SVDquartets and (B) RAxML. Filled circles denote nodes with support values >95%, empty circles denote nodes with support values >90%, and all other nodal support values are indicated as text. Numbered/colored circles enclosing monophyletic groups in the trees indicate species as identified by PTP when applied to the best tree identified by RAxML. Support for these species are as follows: 1) 44%, 2) 82%, 3) 50%. Low support values for the HNG are due to zero branch lengths (see Fig. S4; see Data Accessibility). Corresponding circles are similarly shown on the tree inferred by SVDquartets. However, PTP was not applied to this phylogeny as SVDquartets does not yet infer branch lengths. See Data Accessibility for tree files.

owing to the low number of substitutions observed within species using the reduced dataset for RAxML (excluding heterozygous sites). Specifically, we recovered the following as species: southern Appalachians (82%), northern Appalachians/BRE (44%), and the HNG (50%). The low support for the HNG is almost certainly a consequence of there being zero-value branch lengths separating the two samples. This limits the ability of PTP to test hypotheses that the substitution process differs within and among species. Analysis of a phylogeny inferred by RAxML without an ascertainment bias (and thus including heterozygous sites) confirms this. Doing so, we identified three species with support values greater than 50% (Fig. S4; see Data Accessi-

bility): southern Appalachians (97%), northern Appalachians (57%), and the HNG (95%).

**Species description.**—Herein we describe the Hickory Nut Gorge lineage as a distinct species on the basis of molecular and preliminary morphological differentiation. We adopt the use of subgenus *Castaneides* (Dubois and Raffaëlli, 2012) when referring to the species complex of green salamanders, as this etymology was initially established to refer to eastern *Aneides* which was thought to harbor at least three cryptic species.

***Aneides (Castaneides) caryaensis*, new species**

urn:lsid:zoobank.org:act:99D016DA-6505-4787-BEEB-430C9834F530

Hickory Nut Gorge Green Salamander

Figures 4, S5; Tables 4, S3

**Holotype.**—NCSM 33389, adult male, USA, North Carolina, Rutherford County, from near Bat Cave (exact location withheld due to conservation concerns), 537 m elevation, J. R. Bailey, 22 June 1962.

**Paratypes.**—Herein, exact location data for populations other than the holotype of *A. aeneus* are withheld due to conservation concerns. USNM 446474, same data as holotype; MVZ 178584–178585, North Carolina, Henderson County, A. Westerman, 1 October 1981; NCSM 33389–33391, North Carolina, Rutherford County, just E. of Henderson Co. line on north side of river, across from Bat Cave, near Bat Cave (ca. 1.9 air miles WNW Chimney Rock), J. R. Bailey, 22 June 1962.

**Diagnosis.**—A member of the clade and genus *Aneides*, subgenus *Castaneides*, distinguished from the only other member of the subgenus, *A. (C.) aeneus*, by DNA sequence and preliminary morphological differences. Broadly similar in morphology to *A. aeneus* but differing in some aspects of coloration and in having 1) broader and elongated heads, 2) a greater number of maxillary and premaxillary teeth, 3) limbs that are slightly longer in relation to size, 4) broader shoulders, and 5) broader feet and longer toes.

**Description.**—Slender, very long-legged species of moderate size (maximum known standard length, SL, female 59.8 mm) with slender, whip-like tail (0.93–1.07 SL; longest in male holotype for which tail appears to have regenerated very early in life) and very long digits (longest toe 4.4 mm). Standard lengths (SL) of three sexually mature males are 48.5, 52.4, and 58.4 mm; four females are 52.8, 57.8, 58.9, and 59.8 mm. Head and body are strongly flattened; legs typically extended directly lateral from body. Long limbs overlap by 2.5 to 4 costal interspaces when adpressed to the sides of trunk. Head relatively broad (0.17–0.19, mean 0.18 SL); adductor muscles of jaw bulge outward behind eyes, slightly more in males than in females. Eyes large and prominent. Premaxillary teeth slightly enlarged in relation to those of plethodontids excluding other *Aneides*; in males teeth penetrate upper lip. Maxillary teeth are in short row; posterior portion of maxillary bone is edentulous (as in fig. 2 of Wake, 1963). Anterior vomerine teeth in concave rows of medium length. Posterior vomerine teeth numerous, organized into unified patch on the roof of mouth. Mandibular teeth borne on dentary bone include two to five very large,

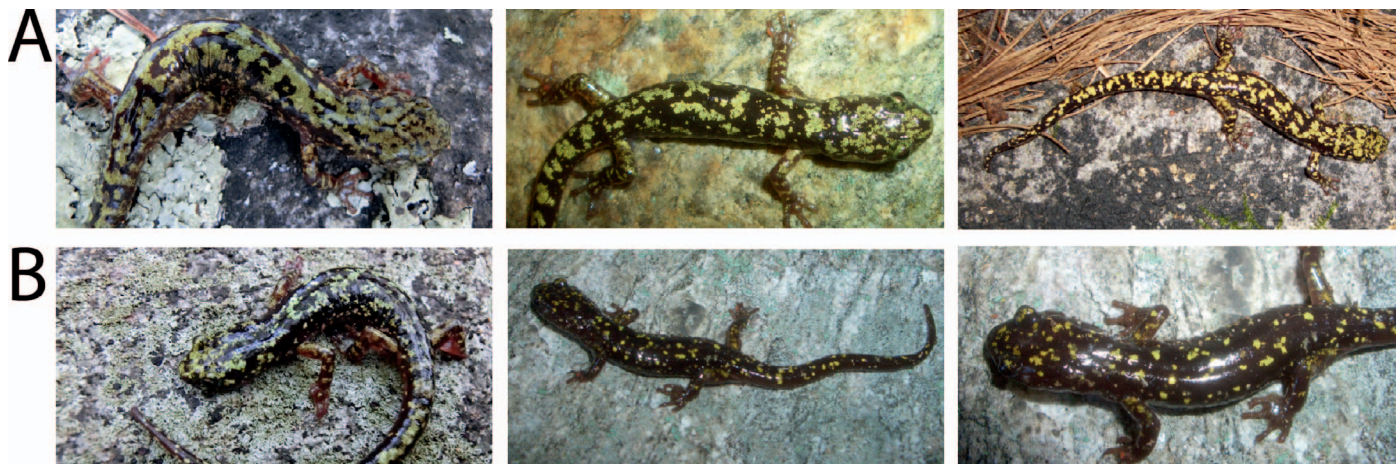


**Fig. 4.** Images representing *Aneides aeneus* (A) and *A. caryaensis* (B). *Aneides caryaensis* is characterized by smaller and less connected lichen-like patches of bright green to yellowish-green pigment.

conical, recurved teeth; other teeth small to moderate in size. Premaxillary teeth number range from three to seven in males, five to 17 in females. Maxillary teeth totals are 12 to 15 in males, 11 to 24 in females. Very small anterior vomerine teeth totals range from six to 17 in males and 12 to 19 in females. Only potential sexual dimorphism noted is somewhat higher tooth numbers in females and slightly larger jaw muscles in males.

**Measurements (in mm), limb interval, and tooth counts of the male holotype.**—SL 58.4, TL 62.6, HW 10.7, SG 15.0, HD 4.5, EL 3.5, EW 1.9, ES 3.8, ED 2.7, EN 3.1, IC 5.6, IO 3.4, SF 20.6, IN 3.0, SP 1.1, SW 6.6, SAV 53.8, AX 29.2, LI -4, CG 14, FLL 17.4, HLL 21.0, HAW 6.7, FW 8.8, T3 4.4, T5 3.2, TP 1.1, TW 3.6, TD 3.2. No mental gland evident. MT 8–7, DT 8 (4 large)–6 (5 large), VT 6–9, PMT 3.

**Coloration in life.**—Ground color of dorsal surfaces is dark brownish-black. Dorsum covered by lichen-like patches of bright green to yellowish-green pigment. Flanks do not have dark pigment as in *A. aeneus*; instead have light grayish-yellow ground color on flanks and venter with loose suffusion of punctate melanophores. Density of punctate melanophores decreases on venter, especially near midline, so venter appears much lighter than other surfaces.

**Comparisons.**—Six adult males range from 49.9 to 55.3 mm SL (mean 52.8), similar to the three males of the new species (48.5–58.4, mean 53.1 mm); three adult females ranged from 44.8 and 53.0 mm (mean 49.5 mm), compared with the somewhat larger females of the new species (52.8–59.8, mean 57.3 mm). Some additional individuals from the Fort Payne area are mature at even smaller sizes; mental glands are present on males as small as 47.3 SL; a specimen from near

**Table 4.** Means of untransformed morphological characters for each *Aneides aeneus* and *A. caryaensis*. Sample sizes are indicated for each species, as are the results of a two-tailed t-test comparing means among species assuming heteroscedasticity. As with our analysis using PCA and LDA, data were normalized where possible and necessary (longest toe, 5<sup>th</sup> toe log transformed; adpressed limbs converted to absolute value and then log transformed). Units are specified below the character being measured. Standard deviations are reported alongside means. Comparisons were made among untransformed characters.

Trait	<i>Aneides aeneus</i> (n = 9)	<i>Aneides caryaensis</i> (n = 7)	T-test P-value
Snout to vent (mm)	51.70±3.02	55.51±4.27	0.072
Axilla to groin (mm)	25.98±1.62	27.16±2.11	0.247
Head width (mm)	8.69±0.74	10.01±0.83	0.006
Forelimb (mm)	14.53±0.88	16.21±1.09	0.006
Hindlimb (mm)	17.08±1.4	18.84±1.42	0.027
Longest toe (mm)	3.39±0.27	3.87±0.42	0.018
5 <sup>th</sup> toe (mm)	2.36±0.11	2.89±0.37	0.007
Costal grooves (count)	14.00±0	14.14±0.38	0.356
Adpressed limbs (# costal interspaces overlapped by adpressed limbs)	-2.11±0.33	-3.36±0.56	<0.001
Snout to gular fold (mm)	12.77±0.88	14.07±0.79	0.008
Tail (mm)	54.14±5.22	56.08±5.45	0.586
Premaxillary teeth (count)	5.56±2.01	9.17±4.31	0.048
Maxillary teeth (count)	9.00±2.65	15.67±4.97	0.005
Vomerine teeth (count)	12.44±3.24	14.14±4.45	0.575
Foot width (mm)	6.91±0.54	7.96±0.82	0.016
Shoulder width (mm)	5.46±0.5	6.50±0.63	0.004
Eye–nostril (mm)	2.67±0.15	2.97±0.17	0.003
Eye–snout (mm)	3.69±0.39	4.07±0.39	0.071

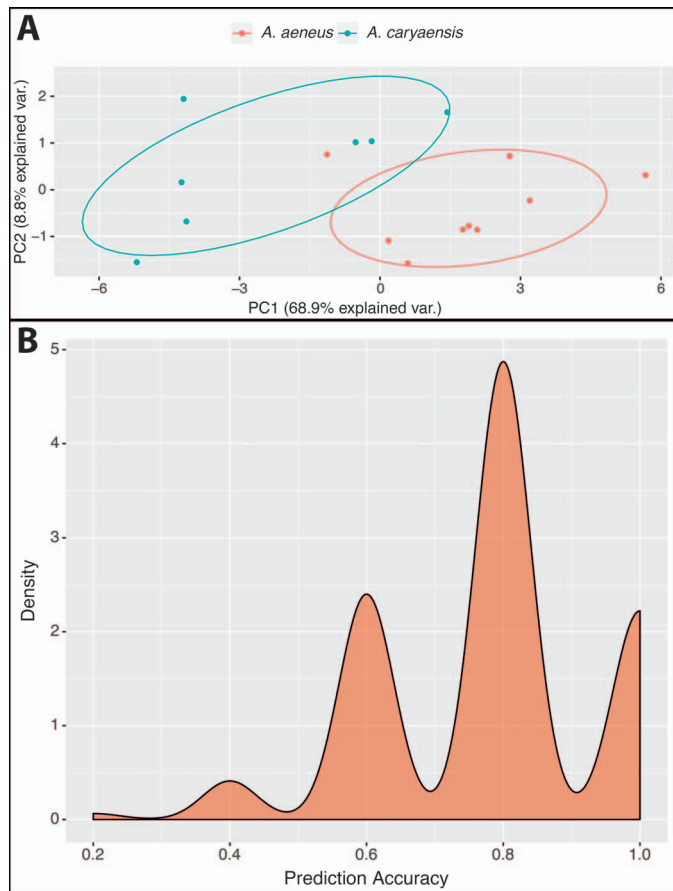


**Fig. 5.** Results of Principal Components Analysis (PCA) and Linear Discriminant Analysis (LDA) using 14 morphological characters. For both analyses, data were normalized where possible and necessary (longest toe, 5<sup>th</sup> toe log-transformed; adpressed limbs converted to absolute value and then log-transformed). (A) PCA with points and normal data ellipses colored by species. (B) Density plot of prediction accuracy by LDA across 1,000 permutations of samples for the training and prediction sets.

Bat Cave has male cloacal morphology at 43.9 SL but no mental gland. These two populations are both near the southern limit of the genus in eastern North America. It thus appears that southern populations of *Castaneides* are smaller, on average, than more northern ones because *A. aeneus* is reported to reach 140 mm total length (the species occurs as far north as south-central Pennsylvania (39.97°N) and as far south as west central Alabama (at least to 32.75°N; Petranks, 1998; AmphibiaWeb, 2018). Juterbock (1989) reports males as large as 65.5 SL and females 65 SL in extreme southern Ohio.

The limbs are relatively longer in *A. caryaensis* relative to *A. aeneus*; combined limb length is 0.63–0.67 SL (mean 0.65) in males and 0.61–0.62 SL (mean 0.62) in females, compared to 0.60–0.65 SL (mean 0.62) in males and 0.58–0.62 SL (mean 0.60) in females of the Fort Payne sample of *A. aeneus*. Additionally, the adpressed limbs cover 2.5 to 4 costal folds in the new species, in contrast to 1.5 to 2.5 in the Fort Payne (*A. aeneus*) sample. All specimens of the new species and of our Fort Payne sample have 14 costal grooves, which means that they have a high likelihood of having 15 trunk vertebrae. Wake (1963) reported counts of 15 (two specimens), 16 (10 specimens), and 17 (4 specimens) trunk vertebrae in individuals from across the range of *A. aeneus*.

Numbers of teeth are broadly similar in the two species. In *A. aeneus*, number of premaxillary teeth ranges from 3–9 and number of vomerine teeth ranges from 8–19. In *A. caryaensis*, number of premaxillary teeth ranges from 5–17 and number of vomerine teeth ranges from 6–19. Number of maxillary teeth differs among species, with *A. aeneus* possessing between 5 and 13, whereas *A. caryaensis* possesses between 11 and 24. This increase in the number of maxillary teeth in *A. caryaensis* relative to *A. aeneus* corresponds to a lengthening and widening of the head (Table 4).

*Aneides caryaensis* is morphologically cryptic in relation to *A. aeneus* according to our preliminary analyses. However, there exist several notable differences among the two species (Table 4; Fig. S5; see Data Accessibility). Outside of coloration differences (Fig. 4), *A. caryaensis* possesses wider and longer heads (perhaps associated with more hypertrophied jaws), longer toes, as well as wider feet and bodies (Table 4). In summary, *A. caryaensis* appears broader, albeit not significantly longer in total length (Table 4). Notably, both PCA and LDA indicate that the two species are morphologically differentiated (Fig. 5) using our preliminary data. A great amount of variance (68.9%) was explained by PC1, with an additional 8.8% explained by PC2 (Fig. 5A). No one variable loaded most heavily onto PC1, however. Our permutation procedure for LDA revealed that we are able to distinguish among species, on average, with 79% prediction accuracy (Fig. 5B).

**Habitat and geographic range.**—Observations recorded by the collector of the holotype, Joseph R. Bailey (field notes stored in North Carolina State Museum) include the following: “June 22, 1962.—about 5–9 PM. Weather warm and fair. Conditions fairly moist.” Specimens collected “just above road on north side of [Broad] river in tight rock crevices in late afternoon. Only a few suitable crevices here. One individual taken at night from rock face on opposite side of river in [*Plethodon*] *longicrus* area. When tickled into sack below it, it flattened against rock and it was necessary to pry it off in contrast to *longicrus* of same size which would drop off.”

**Co-occurring species.**—Three other plethodontid salamander species are commonly encountered in syntopy with *A. caryaensis*: *Plethodon amplus* (*Plethodon jordani* species complex), *Desmognathus cf. carolinensis* (possible intergrade with *Desmognathus ocoee*), and a species that occurs in micro-sympatry and is currently assigned to *Plethodon yonahlossee*, but that was described originally as *Plethodon longicrus* (Adler and Dennis, 1962). Importantly, the type locality of *A. caryaensis* (the Hickory Nut Gorge) is also the type locality of *P. longicrus*. It is noteworthy that these three species are either endemic to the range of *A. caryaensis* or are differentiated to the extent that they either were once recognized as distinct taxa or are currently of undetermined status.

**Etymology.**—Named after the Hickory Nut Gorge of Western North Carolina to which the species is restricted. We allude to this locality by referencing the genus Hickory (*Carya*), after which the locality is named.

## DISCUSSION

In this study, we integrated population genetic, phylogenetic, preliminary morphological, and species delimitation approaches to delimit cryptic species in the green salamander

complex (*A. aeneus*). We find strong, consistent support for the recognition of the Hickory Nut Gorge lineage as a unique species. There is also strong support for the recognition of up to three other lineages (Figs. 2, 3). However, provided the undetermined boundaries between the northern and southern populations, which apparently overlap geographically, we recommend that these be recognized and managed as evolutionarily significant units (ESUs) for the purposes of status assessments and conservation actions, and that further research be conducted to analyze the validity of these lineages as full species.

Our phylogenies, both mitochondrial and nuclear, are concordant with previous research (Sessions and Kezer, 1987) that identifies distinct lineages within the *A. aeneus* complex. Our mitochondrial phylogenetic analysis supports the recognition of *A. caryaensis* as sister to all other members of this complex, sharing common ancestry with other lineages an estimated 12 MYA. That said, these estimates must be regarded as overestimates of the divergence times among these three species, as coalescent times (inferred in the present study) are necessarily greater than divergence times (Nielsen and Slatkin, 2013).

In addition to the strong topological support, a visualization of the geographical distribution of our samples revealed the allopatric distribution of each lineage (Fig. 2). Further, each lineage is geographically assorted with the exception of the contact zone of the northern and southern clades. Comparable levels of cryptic differentiation have also been recently delimited within formerly widespread species complexes in western *Aneides* (Reilly and Wake, 2015; Reilly et al., 2015), and, like *A. aeneus*, the ambiguous nature of these secondary contact zones in both eastern and western U.S. mountain ranges seems to be driven by the complex geologic history of tectonic activity, which we discuss below. In addition to the evidence presented earlier, molecular species delimitation methods consistently and strongly support the recognition of *A. caryaensis* as a distinct species.

We find *A. caryaensis* to be sister to the *A. aeneus* complex, the product of an ancient divergence that was followed by further population subdivision in the remainder of the complex. More detailed sampling will be required to elucidate the phylogenetic history of the complex as a whole. Accordingly, in combination with our population genetic, phylogenetic, and preliminary morphological analyses, we have formally described *A. caryaensis* as a distinct species. Although populations from the Hickory Nut Gorge occur within ~25 km of populations in the Blue Ridge Escarpment, there are high levels of microsatellite differentiation (Table 2), indicating minimal gene flow. This is consistent with other members of Plethodontidae found within the Hickory Nut Gorge. For example, *P. amplus* is endemic to the Hickory Nut Gorge and a distinct form of *P. yonahlossee* that displays genetic and morphological differentiation is found within the Hickory Nut Gorge (Guttman et al., 1978; Highton and Peabody, 2000; Apodaca, unpubl. data). Formal recognition of *A. caryaensis* is urgent considering its small geographic distribution, which is estimated to be approximately 3,625 ha (~35 sq. km) and comprises fewer than 25 known localities. Further, the recent population declines (Corser, 2001) of the nearby BRE lineage and the intensifying human footprint within the Hickory Nut Gorge imply that *A. caryaensis* may be facing similar risks of decline.

**Zoogeography of *Castaneides*.**—Arachnologists (Catley, 1994) have long recognized the striking similarities between

salamanders in *Aneides* and syntopic rock outcrop-inhabiting relict lampshade spiders (*Hypochilus*). These ecologically comparable species (=cryophilic syndrome) share allopatric, disjunct portions of their range in California and the southern Rockies, as well as five eastern species having closely overlapping distributions with eastern *Aneides*. This includes *H. coylei* confined to the Hickory Nut Gorge, a microendemic spider described on subtle genital characters (Huff and Coyle, 1992) and molecularly upheld by Keith and Hedin (2012) as a sister clade to the Cumberland Plateau *H. thorelli*. *Hypochilus coylei* may have shared a common Miocene ancestor with a formerly more widely and easterly distributed *H. thorelli* (Catley, 1994; Hedin, 2001), and similar dynamics may have accounted for the circumscription of *A. caryaensis* within a single valley on the very edge of the southeastern Highlands. Additionally, the previously described species *P. longicrus* (now *P. yonahlossee*) and *P. amplus* are restricted to the Hickory Nut Gorge and surrounding Swannanoa Mountains as well. Although it is unclear at present whether *P. longicrus* is a distinct species or simply a color morph of *P. yonahlossee*, it seems apparent that whatever led to the diversification of *A. caryaensis* in the Hickory Nut Gorge also affected a number of other species.

We have noted that no obvious surface barrier separates the lower elevation populations of *A. caryaensis* from those in BRE, occurring just 25 km to the west (Figs. 1, 2). However, three Mesozoic-aged faults (Snipes et al., 1986) lie precisely in the region between *A. caryaensis* and the BRE clade and *H. coylei*/*H. pococki*. These lower hills are known as the Hendersonville bulge and lie just east of the Brevard fault zone—the generalized physiographic edge of the Blue Ridge province—belonging geologically to the lower relief of Piedmont Province (Hack, 1982). Rejuvenated global and Appalachian Miocene uplift 10–20 MYA (Gallen et al., 2013; Liu, 2014) altered the climate and ecosystems towards a more grassland-dominated terrestrial ecosystem at the expense of the mixed mesophytic forests (Kürschner et al., 2008). The faults are thought to have been the loci of small differential movements, most recently during the late Miocene ~12 MYA that affected the gross morphology of the terrain sufficiently to act as a barrier to gene flow for these rather sedentary species (Hack, 1982; Gallen et al., 2013).

It is possible that *Castaneides* previously had a more easterly Piedmont distribution which subsequently was lost as forests retreated to protected upland gorges after the Miocene optimum ~15 MYA (Kürschner et al., 2008). This hypothesis could explain why these salamander and spider populations became relictualized in the outlying Hickory Nut Gorge, surrounded as they are to the west by a much more mountainous terrain housing widespread congeners but which became extensively fragmented in the southern uplands. This scenario predicts the existence of another forested refuge on the southern Cumberland Plateau, and it was from here that the remainder of the *Castaneides* were subsequently founded as forest cover waxed and waned since the late Miocene. Martin et al.'s (2016) ancestral area analysis also hinted that the ancestor of *Castaneides* might have been a more widespread lowland and potentially arboreal form.

**Karyotypic variation.**—*Aneides* differs from other plethodontid genera in the extent of chromosomal variation (Sessions and Kezer, 1987). With few exceptions, plethodontids have 13 or 14 pairs of biarmed chromosomes and closely resemble each other. While all species of *Aneides* have 14 pairs of chromosomes, at least eight distinct karyotypes are found,

three of them in the *A. aeneus* complex. One of these is “Morescalchi’s *aeneus* III” (Sessions and Kezer, 1987), potentially important taxonomically but unavailable because of the lack of detailed geographic information (obtained by long-deceased Morescalchi from an unnamed animal dealer and suspected of being from the vicinity of Cumberland County, Tennessee). Morescalchi’s materials, stored in Italy, were destroyed in the Naples earthquake in 1980. This region lies between sites where “*aeneus* I” (to the north) and “*aeneus* II” (to the southwest) have been recorded. In their map (fig. 13), Sessions and Kezer (1987) show *aeneus* I and II in sympatry (p. 24: “at one locality, near Chattanooga, Tennessee, a single specimen with the *aeneus* I karyotype has been detected among mainly *aeneus* II individuals”). A specimen from Hickory Nut Gorge has the *aeneus* I karyotype.

The report of Sessions and Kezer (1987) suggests that three karyotypes are found in eastern Tennessee, two of them in sympatry. In a recent communication to DBW (29 May 2018), Sessions provided additional details and corrected errors. For the published study, he examined three specimens of *A. aeneus* from “near Chattanooga”, which he now specifies as from 4 miles S Sherwood at Buck Creek Cove, Franklin Co., Tennessee (collected by Wayne Van Devender). This site is just a few km west of Nickajack Cave (now mainly inundated by a reservoir), the type locality of *A. aeneus*. These specimens were sent to Kezer in Eugene, Oregon. Sessions took one to Berkeley, California, for his studies, and Kezer examined the other two. In a letter to Sessions (dated 29 November 1981), Kezer reports that the specimens he examined had completely bi-armed chromosomes (i.e., *aeneus* II). Sessions double-checked his lab notes from the time and finds that his single specimen also was *aeneus* II. He cannot explain how an error was made in the published version, but he concludes: “there was no evidence of co-occurrence of *aeneus* I and II at that site”. Sessions sent DBW a complete list of specimens examined. There were no other specimens from Tennessee, and only the single specimen from Hickory Nut Gorge from North Carolina. They did have specimens from two sites in Alabama, both *aeneus* II. The map in their publication (fig. 13) is accordingly flawed and must be used with extreme care. Importantly for our current work, the specimen from Hickory Nut Gorge is *aeneus* I, which is found only at this site and from Kentucky and Virginia northwards to Maryland and Ohio, and nowhere else in any species of *Aneides* or any other plethodontid. The finding of the *aeneus* I karyotype in Hickory Nut Gorge is important in showing a sharp difference between this region and the region of the type locality of *A. aeneus*, very near the Tennessee–Alabama border.

A cladogram of chromosomal characters in *Aneides* shows the clade differing from the outgroup used (*Plethodon*) in two shared derived traits (Sessions and Kezer, 1987: fig. 15). *Aneides aeneus* differs further from other members of the genus in two more traits, and *aeneus* I and II are sister taxa. Karyotypic differences reported by Sessions and Kezer in the *A. ferreus* complex later proved to be species specific: *ferreus* I = *Aneides ferreus*, and *ferreus* II = *Aneides vagrans* (Jackman, 1998).

**Conservation implications.**—*Aneides caryaensis* faces pressing conservation concerns and need for management. This species has an extremely narrow range and is reported from fewer than 25 localities, despite extensive searches. The status of these populations is unknown, yet based on the

personal observations of several of the authors, densities appear to be very low at all of the known localities, including those that had higher surveyed (by the North Carolina Wildlife Resource Commission) densities, often with only one to three individuals observed during a site visit. Additionally, these field observations are supported by our estimates of genetic diversity (Table 3), which indicate that populations of *A. caryaensis* are experiencing a high amount of inbreeding, a clear signature of small population sizes (Frankham et al., 2010). High levels of inbreeding can have detrimental effects on populations, including a decrease in fecundity that can in turn lead to lower population sizes and increased inbreeding, a feedback cycle often referred to as “the extinction vortex” (Frankham et al., 2010). Habitat loss and fragmentation resulting from the rapid rate of tourism, real estate development, and transportation and energy infrastructure within the Hickory Nut Gorge is likely the largest direct threat to the long-term survival of *A. caryaensis*. Habitat fragmentation and loss can easily occur for this species, as habitat features preferred by *A. caryaensis* tend to be distributed in patches across the landscape and are susceptible to disturbance from anthropogenic activities.

Similar to *A. caryaensis*, the BRE populations of *A. aeneus* also face a myriad of threats and conservation concerns. Although some populations in the BRE appeared to be recovering from the dramatic (98%) declines of the 1980s and 90s (Corser, 2001), they have been experiencing declines since at least 2005 (Apodaca and Williams, unpubl. data). The low present-day diversity observed for the BRE populations included in our study (Table 3) seems to reflect these declines. Importantly, the subpopulation structure within the BRE and apparent admixture between subpopulations attests to this complex demographic history. Although we have not explicitly tested demographic hypotheses for the BRE populations, our results imply either 1) secondary contact among previously isolated populations or 2) ongoing divergence. Future work studying the BRE populations would benefit from a thorough investigation of their demographic history.

Regardless, the low present day diversity of these populations in conjunction with their historical and continued declines emphasizes a great need to conserve and manage current populations and to develop novel approaches to mitigate threats. Necessary conservation actions will involve 1) protecting areas of known and potential habitat from certain types of logging, development, and collecting, and 2) maintaining a permeable matrix of habitat between such areas to facilitate dispersal.

In accordance with the mitochondrial and nuclear distinctiveness of this lineage, we propose the recognition of the BRE lineage of the *A. aeneus* complex as an ESU. This proposal is compatible with the criterion for recognizing ESUs outlined by Moritz (1994). In his article, Moritz (1994) defined an ESU as being “reciprocally monophyletic for mtDNA alleles and show significant divergence of alleles at nuclear loci.” We have demonstrated this for the BRE lineage of *A. aeneus* despite apparent population structuring. Although our OTU sampling for the SNP dataset is far less than that of our mitochondrial dataset, we have recovered reciprocal monophyly for the BRE populations. Further, the BRE lineage, as identified herein, is compatible with a number of other definitions of ESUs as outlined by Funk et al. (2012; e.g., Avise, 1994; Vogler and DeSalle, 1994; Fraser and Bernatchez, 2001). As such, we anticipate our recommendation for the recognition of the BRE populations of *A.*

*aeneus* as an ESU to be uncontentious. Recognition of the BRE lineage as an ESU will facilitate its conservation, as ESUs are granted legal protection under the Endangered Species Act. We do note, however, that species delimitation methods included BRE populations with northern Appalachian lineages (Fig. 3). Interestingly, the PTP designated the southern Appalachian lineage as a distinct species. This is coincident with long branch-lengths as estimated by RAxML. Too little is known about these populations at present to designate this lineage as an ESU, but we anticipate that additional investigation of this lineage will uncover previously unrecognized differentiation.

**Conclusions.**—Herein, we have used multiple lines of evidence to identify four lineages within *Castaneides*. The newly described North Carolina endemic, *A. caryaensis*, is restricted to an extremely narrow geographic range and is in need of immediate protection. However, little is known about the ecology of this species, as most work done on *Castaneides* has been conducted on more westerly populations and the Blue Ridge Escarpment lineage (e.g., Gordon, 1952; Snyder, 1983, 1991; Cupp, 1991; Corser, 2001; Waldron and Humphries, 2005; Smith et al., 2017). Perhaps the most important research needs at present are population surveys, habitat management guidelines, landscape genetic analyses, and habitat use studies. We emphasize, however, that such research needs are not restricted to *A. caryaensis*. The BRE ESU of *A. aeneus* is also of great conservation concern and faces similar threats as *A. caryaensis*. In summary, we hope that in describing *A. caryaensis*, more work will be conducted to more rigorously describe the cryptic diversity harbored within *Castaneides*.

#### DATA ACCESSIBILITY

Supplemental information is available at <https://www.copeiajournal.org/ch-18-052>.

#### ACKNOWLEDGMENTS

We are deeply indebted to D. Rupp and C. McGrath for historical inventories of the Hickory Nut Gorge and to W. Smith for tissue collection. We would also like to thank M. Olszack, K. Berrier, K. Curtis, and K. Crandall for conducting genetics laboratory work. Stacey Lance assisted in developing the microsatellites. K. Jones assisted in museum sample measurements. We are thankful to USNM herpetology and their curators, who provided access to their samples. NC samples were collected under permit number 14-ES00431. AP and JJA contributed equally to the manuscript.

#### LITERATURE CITED

- Adler, K. K., and D. M. Dennis. 1962. *Plethodon longicrus*, a new salamander (Amphibia: Plethodontidae) from North Carolina. Special Publications of the Ohio Herpetological Society 4:1–14.
- Alford, R. A., and S. J. Richards. 1999. Global amphibian declines: a problem in applied ecology. *Annual Review of Ecology and Systematics* 30:133–165.
- AmphibiaWeb. 2018. <https://amphibiaweb.org>. University of California, Berkeley, CA, USA (accessed 15 November 2018).
- Avise, J. C. 1994. *Molecular Markers, Natural History and Evolution*. Chapman and Hall, New York.
- Becker, C. G., C. R. Fonseca, C. F. B. Haddad, R. F. Batista, and P. I. Prado. 2007. Habitat split and the global decline of amphibians. *Science* 318:1775–1777.
- Bogart, J. P., and M. Tandy. 1976. Polyploid amphibians: three more diploid-tetraploid cryptic species of frogs. *Science* 193:334–335.
- Bouckaert, R., J. Heled, D. Kühnert, T. Vaughan, C.-H. Wu, D. Xie, M. A. Suchard, A. Rambaut, and A. J. Drummond. 2014. BEAST 2: a software platform for Bayesian evolutionary analysis. *PLoS Computational Biology* 10: e1003537.
- Camp, C. D., and J. A. Wooten. 2016. Hidden in plain sight: cryptic diversity in the Plethodontidae. *Copeia* 104:111–117.
- Carlsson, J. 2008. Effects of microsatellite null alleles on assignment testing. *Journal of Heredity* 99:616–623.
- Castoe, T. A., A. W. Poole, A. J. de Koning, K. L. Jones, D. F. Tombback, S. J. Oyler-McCance, J. A. Fike, S. L. Lance, J. W. Streicher, E. N. Smith, and D. D. Pollock. 2012. Rapid microsatellite identification from Illumina paired-end genomic sequencing in two birds and a snake. *PLoS ONE* 7:e30953.
- Catley, K. M. 1994. Descriptions of new *Hypochilus* species from New Mexico and California: with a cladistic analysis of the Hypochilidae (Araneae). *American Museum Novitates* 3088:1–27.
- Chapuis, M. P., and A. Estoup. 2007. Microsatellite null alleles and estimation of population differentiation. *Molecular Biology and Evolution* 24:621–631.
- Chen, C., E. Durand, F. Forbes, and O. François. 2007. Bayesian clustering algorithms ascertaining spatial population structure: a new computer program and a comparison study. *Molecular Ecology Notes* 7:747–756.
- Cherty, L. M., S. M. Case, and A. C. Wilson. 1978. Frog perspective on the morphological difference between humans and chimpanzees. *Science* 200:209–211.
- Chifman, J., and L. Kubatko. 2014. Quartet inference from SNP data under the coalescent model. *Bioinformatics* 30: 3317–3324.
- Collins, J. P., and A. Storfer. 2003. Global amphibian declines: sorting the hypotheses. *Diversity and Distributions* 9:89–98.
- Corser, J. D. 2001. Decline of a disjunct green salamander (*Aneides aeneus*) populations in the southern Appalachians. *Biological Conservation* 97:119–126.
- Cupp, P. V. 1991. Aspects of the life history and ecology of the Green Salamander, *Aneides aeneus*, in Kentucky. *Journal of the Tennessee Academy of Science* 66:171–174.
- Danecek, P., A. Auton, G. Abecasis, C. A. Albers, E. Banks, M. A. DePristo, R. E. Handsaker, G. Lunter, G. T. Marth, S. T. Sherry, and G. McVean. 2011. The variant call format and VCFtools. *Bioinformatics* 27:2156–2158.
- Darriba, D., G. L. Taboada, R. Doallo, and D. Posada. 2012. jModelTest2: more models, new heuristics and parallel computing. *Nature Methods* 9:772.
- De Queiroz, K. 2007. Species concepts and species delimitation. *Systematic Biology* 56:879–886.
- Dirzo, R., H. S. Young, M. Galetti, G. Ceballos, N. J. B. Isaac, and B. Collen. 2014. Defaunation in the Anthropocene. *Science* 345:401–406.
- Drummond, A. J., and R. R. Bouckaert. 2015. *Bayesian evolutionary analysis with BEAST 2*. Cambridge University Press, U.K.

- Dubois, A., and J. Raffaëlli. 2012. A new ergotaxonomy of the order Urodela Duméril, 1805 (Amphibia, Batrachia). *Alytes* 28:77–161.
- Eaton, D. A. R., and I. Overcast. 2016. ipyrad: interactive assembly and analysis of RADseq data sets. <https://ipyrad.readthedocs.io/> (accessed October 2017).
- Elmer, K. R., R. M. Bonett, D. B. Wake, and S. C. Lougheed. 2013. Early Miocene origin and cryptic diversification of South American salamanders. *BMC Evolutionary Biology* 13:59.
- Eschbach, E., and S. Schöning. 2013. Identification of high-resolution microsatellites without a priori knowledge of genotypes using a simple scoring approach. *Methods in Ecology and Evolution* 4:1076–1082.
- Excoffier, L., and G. Laval. 2005. Arlequin (version 3.0): an integrated software package for population genetics data analysis. *Evolutionary Bioinformatics Online* 1:47–50.
- François, O., and E. Durand. 2010. Spatially explicit Bayesian clustering models in population genetics. *Molecular Ecology Resources* 10:773–784.
- Frankham, R., J. D. Ballou, and D. A. Briscoe. 2010. *Introduction to Conservation Genetics*. Cambridge University Press, U.K.
- Fraser, D. J., and L. Bernatchez. 2001. Adaptive evolutionary conservation: towards a unified concept for defining conservation units. *Molecular Ecology* 10:2741–2752.
- Funk, W. C., J. K. McKay, P. A. Hohenlohe, and F. W. Allendorf. 2012. Harnessing genomics for delineating conservation units. *Trends in Ecology and Evolution* 27:489–496.
- Gallen, S. F., K. W. Wegmann, and D. R. Bohnenstiehl. 2013. Miocene rejuvenation of topographic relief in the southern Appalachians. *GSA Today* 23:4–10.
- Goebel, A. M., J. M. Donnelly, and M. E. Atz. 1999. PCR primers and amplification methods for 12S ribosomal DNA, the control region, cytochrome oxidase I, and cytochrome b in bufonids and other frogs, and an overview of PCR primers which have amplified DNA in amphibians successfully. *Molecular Phylogenetics and Evolution* 11:163–199.
- Gordon, R. E. 1952. A contribution to the life history and ecology of the plethodontid salamander *Aneides aeneus* (Cope and Packard). *American Midland Naturalist* 47:666–701.
- Guttman, S. I., A. A. Karlin, and G. M. Labanick. 1978. A biochemical and morphological analysis of the relationship between *Plethodon longicrus* and *Plethodon yonahlossee* (Amphibia, Urodela, Plethodontidae). *Journal of Herpetology* 12:445–454.
- Hack, J. T. 1982. Physiographic divisions and differential uplift in the Piedmont and Blue Ridge. U.S. Geological Survey Professional Paper No. 1265.
- Hammerson, G. 2004. *Aneides aeneus*. The IUCN Red List of Threatened Species 2004. <http://dx.doi.org/10.2305/IUCN.UK.2004.RLTS.T1282A3385547.en>.
- Hammerson, G., and F. Dirrigl. 2017. *Aneides aeneus* - (Cope and Packard, 1881) Green Salamander. NatureServe <http://explorer.natureserve.org/servlet/NatureServe?searchName=aneides+aeneus>.
- Hedin, M. C. 2001. Molecular insights into species phylogeny, biogeography, and morphological stasis in the ancient spider genus *Hypochilus* (Araneae: Hypochilidae). *Molecular Phylogenetics and Evolution* 18:238–251.
- Highton, R. 1995. Speciation in eastern North American salamanders of the genus *Plethodon*. *Annual Review of Ecology and Systematics* 26:579–600.
- Highton, R. 1999. Geographic protein variation and speciation in the salamanders of the *Plethodon cinereus* group with the description of two new species. *Herpetologica* 55:43–90.
- Highton, R., G. C. Maha, and L. R. Maxson. 1989. Biochemical evolution in the slimy salamanders of the *Plethodon glutinosus* complex in the eastern United States. *Illinois Biological Monographs* 57. University of Illinois Press, Urbana and Chicago, Illinois.
- Highton, R., and R. B. Peabody. 2000. Geographic protein variation and speciation in salamanders of the *Plethodon jordani* and *Plethodon glutinosus* complexes in the southern Appalachian Mountains with the description of four new species, p. 31–93. *In: The Biology of Plethodontid Salamanders*. R. C. Bruce, R. G. Jaeger, and L. D. Houck (eds.). Springer, Boston.
- Hillis, D. M., J. S. Frost, and D. A. Wright. 1983. Phylogeny and biogeography of the *Rana pipiens* complex: a biochemical evaluation. *Systematic Zoology* 32:132–143.
- Huff, R. P., and F. A. Coyle. 1992. Systematics of *Hypochilus sheari* and *Hypochilus coylei*, two southern Appalachian lampshade spiders (Araneae, Hypochilidae). *Journal of Arachnology* 20:40–46.
- Jackman, T. R. 1998. Molecular and historical evidence for the introduction of clouded salamanders (genus *Aneides*) to Vancouver Island, British Columbia, Canada, from California. *Canadian Journal of Zoology* 76:1570–1580.
- Jia, F., N. Lo, and S. Y. Ho. 2014. The impact of modelling rate heterogeneity among sites on phylogenetic estimates of intraspecific evolutionary rates and timescales. *PLoS ONE* 9:e95722.
- Jockusch, E. L., and D. B. Wake. 2002. Falling apart and merging: diversification of slender salamanders (Plethodontidae: *Batrachoseps*) in the American West. *Biological Journal of the Linnean Society* 76:361–391.
- Juterbock, J. E. 1989. *Aneides aeneus* (Cope and Packard) green salamander, p. 189–195. *In: Salamanders of Ohio*. R. A. Pfingstin and F. L. Downs (eds.). Ohio Biological Survey Bulletin, New series Volume 7, Number 2.
- Kearse, M., R. Moir, A. Wilson, S. Stones-Havas, M. Cheung, S. Sturrock, S. Buxton, A. Cooper, S. Markowitz, C. Duran, T. Thierer, B. Ashton, P. Meintjes, and A. Drummond. 2012. Geneious Basic: an integrated and extendable desktop software platform for the organization and analysis of sequence data. *Bioinformatics* 28:1647–1649.
- Keith, R., and M. Hedin. 2012. Extreme mitochondrial population subdivision in southern Appalachian paleoendemic spiders (Araneae: Hypochilidae: Hypochilus), with implications for species delimitation. *Journal of Arachnology* 40:167–181.
- Koressaar, T., and M. Remm. 2007. Enhancements and modifications of primer design program Primer3. *Bioinformatics* 23:1289–1291.
- Kotsakiozi, P., D. Jablonski, Ç. Ilgaz, Y. Kumlutaş, A. Avcı, S. Meiri, Y. Itescu, O. Kukushkin, V. Gvoždík, G. Scillitani, and S. A. Roussos. 2018. Multilocus phylogeny and coalescent species delimitation in Kotschy's gecko, *Mediodactylus kotschy*: hidden diversity and cryptic species. *Molecular Phylogenetics and Evolution* 125:177–187.
- Kozak, K. H., D. W. Weisrock, and A. Larson. 2006. Rapid lineage accumulation in a non-adaptive radiation: phylo-

- genetic analysis of diversification rates in eastern North American woodland salamanders (Plethodontidae: *Plethodon*). Proceedings of the Royal Society of London B: Biological Sciences 273:539–546.
- Kozak, K. H., and J. J. Wiens.** 2006. Does niche conservatism promote speciation? A case study in North American salamanders. *Evolution* 60:2604–2621.
- Kozak, K. H., and J. J. Wiens.** 2010. Niche conservatism drives elevational diversity patterns in Appalachian salamanders. *The American Naturalist* 176:40–54.
- Kuchta, S. R., A. D. Brown, and R. Highton.** 2018. Disintegrating over space and time: paraphyly and species delimitation in the Wehrle's Salamander complex. *Zoologica Scripta* 47:285–299.
- Kürschner, W. M., Z. Kvaček, and D. L. Dilcher.** 2008. The impact of Miocene atmospheric carbon dioxide fluctuations on climate and the evolution of terrestrial ecosystems. Proceedings of the National Academy of Sciences of the United States of America 105:449–453.
- Lapointe, F. J., and L. J. Rissler.** 2005. Congruence, consensus, and the comparative phylogeography of codistributed species in California. *The American Naturalist* 166:290–299.
- Leaché, A. D., B. L. Banbury, J. Felsenstein, A. N. M. De Oca, and A. Stamatakis.** 2015. Short tree, long tree, right tree, wrong tree: new acquisition bias corrections for inferring SNP phylogenies. *Systematic Biology* 64:1032–1047.
- Lischer, H. E., and L. Excoffier.** 2011. PGDSpider: an automated data conversion tool for connecting population genetics and genomics programs. *Bioinformatics* 28:298–299.
- Liu, L.** 2014. Rejuvenation of Appalachian topography caused by subsidence-induced differential erosion. *Nature Geoscience* 7:518–523.
- Luo, A., C. Ling, S. Y. Ho, and C. Zhu.** 2018. Comparison of methods for molecular species delimitation across a range of speciation scenarios. *Systematic Biology* 67:830–846.
- Margres, M. J., A. Patton, K. P. Wray, A. T. Hassinger, M. J. Ward, E. M. Lemmon, A. R. Lemmon, and D. R. Rokyta.** 2018. Tipping the scales: the migration–selection balance leans toward selection in snake venoms. *Molecular Biology and Evolution* 36:271–282.
- Martin, S. D., D. B. Shepard, M. A. Steffen, J. G. Phillips, and R. M. Bonett.** 2016. Biogeography and colonization history of plethodontid salamanders from the Interior Highlands of eastern North America. *Journal of Biogeography* 43:410–422.
- Meirmans, P. G., and P. H. van Tienderen.** 2004. GENOTYPE and GENODIVE: two programs for the analysis of genetic diversity of asexual organisms. *Molecular Ecology Notes* 4:792–794.
- Miller, M. A., W. Pfeiffer, and T. Schwartz.** 2010. Creating the CIPRES Science Gateway for inference of large phylogenetic trees. 2010 Gateway Computing Environments Workshop (GCE), New Orleans, Louisiana, 2010.
- Morando, M., L. J. Avila, and J. W. Sites, Jr.** 2003. Sampling strategies for delimiting species: genes, individuals, and populations in the *Liolaemus elongatus-kriegi* complex (Squamata: Liolamidae) in Andean-Patagonian South America. *Systematic Biology* 52:159–185.
- Moritz, C.** 1994. Defining 'evolutionarily significant units' for conservation. *Trends in Ecology and Evolution* 9:373–375.
- Moritz, C., C. J. Hoskin, J. B. MacKenzie, B. L. Phillips, M. Tonione, N. Silva, J. VanDerWal, S. E. Williams, and C. H. Graham.** 2009. Identification and dynamics of a cryptic suture zone in tropical rainforest. Proceedings of the Royal Society B: Biological Sciences 276:1235–1244.
- Moritz, C., C. J. Schneider, and D. B. Wake.** 1992. Evolutionary relationships within the *Ensantina eschscholtzii* complex confirm the ring species interpretation. *Systematic Biology* 41:273–291.
- Mueller, R. L., J. R. Macey, M. Jaekel, D. B. Wake, and J. L. Boore.** 2004. Morphological homoplasy, life history evolution, and historical biogeography of plethodontid salamanders inferred from complete mitochondrial genomes. Proceedings of the National Academy of Sciences of the United States of America 101:13820–13825.
- Myers, N., R. A. Mittermeier, C. G. Mittermeier, G. A. B. de Fonseca, and J. Kent.** 2000. Biodiversity hotspots for conservation priorities. *Nature* 403:853–858.
- Nei, M.** 1987. *Molecular Evolutionary Genetics*. Columbia University Press, New York.
- Nielsen, R., and M. Slatkin.** 2013. *An Introduction to Population Genetics: Theory and Applications*. Sinauer Associates, Inc., Sunderland, Massachusetts.
- Noss, R. F., E. T. LaRoe, and J. M. Scott.** 1995. *Endangered ecosystems of the United States: a preliminary assessment of loss and degradation*. Biological Report 28. U.S. Department of the Interior, National Biological Service, Washington, D.C.
- Pauly, G. B., O. Piskurek, and H. B. Shaffer.** 2006. Phylogeographic concordance in the southeastern United States: the flatwoods salamander, *Ambystoma cingulatum*, as a test case. *Molecular Ecology* 16:415–429.
- Pechmann, J., and H. M. Wilbur.** 1994. Putting declining amphibian populations in perspective: natural fluctuations and human impacts. *Herpetologica* 50:65–84.
- Petranka, J. W.** 1998. *Salamanders of the United States and Canada*. Smithsonian Institution Press, Washington, D.C.
- Pickering, J., R. Kays, A. Meier, and S. Andrew.** 2003. The Appalachians, p. 458–467. *In: Wilderness—Earth's last wild places*. P. R. Gil, R. A. Mittermeier, C. G. Mittermeier, J. Pilgrim, G. Fonseca, W. R. Konstant, and T. Brooks (eds.). Conservation International, Washington, D.C.
- Pons, J., T. G. Barraclough, J. Gomez-Zurita, A. Cardoso, D. P. Duran, S. Hazell, S. Kamoun, W. D. Sumlin, and A. P. Vogler.** 2006. Sequence-based species delimitation for the DNA taxonomy of undescribed insects. *Systematic Biology* 55:595–609.
- Pope, C. H.** 1928. Some plethodontid salamanders from North Carolina and Kentucky, with the description of a new race of *Leurognathus*. *American Museum Novitates* 306:1–19.
- R Core Team.** 2017. R: a language and environment for statistical computing. R Foundation for Statistical Computing, Vienna, Austria. <https://www.R-project.org/>
- Rambaut, A., M. A. Suchard, and A. Drummond.** 2014. Tracer v1.6. <http://beast.bio.ed.ac.uk/Tracer>
- Reilly, S. B., A. Corl, and D. B. Wake.** 2015. An integrative approach to phylogeography: investigating the effects of ancient seaways, climate, and historical geology on multi-locus phylogeographic boundaries of the Arboreal Salamander (*Aneides lugubris*). *BMC Evolutionary Biology* 15: 241.
- Reilly, S. B., and D. B. Wake.** 2015. Cryptic diversity and biogeographical patterns within the black salamander



- (*Aneides flavipunctatus*) complex. *Journal of Biogeography* 42:280–291.
- Rissler, L., and J. Apodaca. 2007. Adding more ecology in species delimitation: ecological niche models and phylogeography help define cryptic species in the black salamander (*Aneides flavipunctatus*). *Systematic Biology* 56:924–942.
- Rissler, L. J., R. J. Hijmans, C. H. Graham, C. Moritz, and D. B. Wake. 2006. Phylogeographic lineages and species comparisons in conservation analyses: a case study of California herpetofauna. *The American Naturalist* 167:655–666.
- Rohland, N., and D. Reich. 2012. Cost-effective, high-throughput DNA sequencing libraries for multiplexed target capture. *Genome Research* 22:939–946.
- Rousset, F. 2008. genepop'007: a complete re-implementation of the genepop software for Windows and Linux. *Molecular Ecology Resources* 8:103–106.
- Rovito, S. M., G. Parra Olea, J. Hanken, R. M. Bonett, and D. B. Wake. 2013. Adaptive radiation in miniature: the minute salamanders of the Mexican highlands (Amphibia: Plethodontidae: *Thorius*). *Biological Journal of the Linnean Society* 109:622–643.
- Roy, V., R. Constantino, V. Chassany, S. Giusti-Miller, M. Diouf, P. Mora, and M. Harry. 2014. Species delimitation and phylogeny in the genus *Nasutitermes* (Termitidae: Nasutitermitinae) in French Guiana. *Molecular Ecology* 23:902–920.
- Rundell, R. J., and T. D. Price. 2009. Adaptive radiation, nonadaptive radiation, ecological speciation and nonecological speciation. *Trends in Ecology and Evolution* 24:394–399.
- Sabaj, M. H. 2016. Standard symbolic codes for institutional resource collections in herpetology and ichthyology: an Online Reference. Version 6.5 (16 August 2016). Electronically accessible at <http://www.asih.org/>, American Society of Ichthyologists and Herpetologists, Washington, D.C.
- Schwarz, G. 1978. Estimating the dimension of a model. *The Annals of Statistics* 6:461–464.
- Sessions, S. K., and J. Kezer. 1987. Cytogenetic evolution in the plethodontid salamander genus *Aneides*. *Chromosoma* 95:17–30.
- Shen, X. X., D. Liang, M. Y. Chen, R. L. Mao, D. B. Wake, and P. Zhang. 2016. Enlarged multilocus data set provides surprisingly younger time of origin for the Plethodontidae, the largest family of salamanders. *Systematic Biology* 65:66–81.
- Smith, W. H., S. L. Slep, C. D. Stanley, M. N. Blackburn, and J. Wayland. 2017. Rock crevice morphology and forest contexts drive microhabitat preferences in the Green Salamander (*Aneides aeneus*). *Canadian Journal of Zoology* 95:353–358.
- Snipes, D. S., P. R. Manoogian, M. W. Davis, L. L. Burnett, J. A. Wylie, and S. B. Heaton. 1986. Ground-water problems in the Mesozoic Pax Mountain Fault zone. *Groundwater* 24:375–381.
- Snyder, D. H. 1983. The apparent crash and possible extinction of the green salamander, *Aneides aeneus*, in the Carolinas. *Association of Southeastern Biologists Bulletin* 30:82.
- Snyder, D. H. 1991. The green salamander (*Aneides aeneus*) in Tennessee and Kentucky with comments on the Carolinas' Blue Ridge populations. *Journal of the Tennessee Academy of Science* 66:165–169.
- Spiegelhalter, D. J., N. G. Best, B. P. Carlin, and A. Van Der Linde. 2002. Bayesian measures of model complexity and fit. *Journal of the Royal Statistical Society: Series B (Statistical Methodology)* 64:583–639.
- Stamatakis, A. 2014. RAxML version 8: a tool for phylogenetic analysis and post-analysis of large phylogenies. *Bioinformatics* 30:1312–1313.
- Stuart, B. L., R. F. Inger, and H. K. Voris. 2006. High level of cryptic species diversity revealed by sympatric lineages of Southeast Asian forest frogs. *Biology Letters* 2:470–474.
- Sukumaran, J., and M. T. Holder. 2010. DendroPy: a Python library for phylogenetic computing. *Bioinformatics* 26:1569–1571.
- Sukumaran, J., and L. L. Knowles. 2017. Multispecies coalescent delimits structure, not species. *Proceedings of the National Academy of Sciences of the United States of America* 114:1607–1612.
- Swofford, D. L. 2003. PAUP\*: phylogenetic analysis using parsimony (\*and other methods). Version 4. Sinauer Associates, Sunderland, Massachusetts.
- Tan, A. M., and D. B. Wake. 1995. MtDNA phylogeography of the California newt, *Taricha torosa* (Caudata, Salamandridae). *Molecular Phylogenetics and Evolution* 4:383–394.
- Thompson, J. D., T. J. Gibson, F. Plewniak, F. Jeanmougin, and D. G. Higgins. 1997. The CLUSTAL\_X Windows interface: flexible strategies for multiple sequence alignment aided by quality analysis tools. *Nucleic Acids Research* 25:4876–4882.
- Titus, B. M., M. Daly, N. Hamilton, M. L. Berumen, and J. A. Baeza. 2018. Global species delimitation and phylogeography of the circumtropical 'sexy shrimp' *Thor amboinensis* reveals a cryptic species complex and secondary contact in the Indo-West Pacific. *Journal of Biogeography* 45:1275–1287.
- Untergasser, A., I. Cutcutache, T. Koressaar, J. Ye, B. C. Faircloth, M. Remm, and S. G. Rozen. 2012. Primer3—new capabilities and interfaces. *Nucleic Acids Research* 40:e115.
- Vogler, A. P., and R. DeSalle. 1994. Diagnosing units of conservation management. *Conservation Biology* 8:354–363.
- Wake, D. B. 1963. Comparative osteology of the plethodontid salamander genus *Aneides*. *Journal of Morphology* 113:77–118.
- Wake, D. B. 1991. Homoplasy: the result of natural selection or evidence of design limitations? *American Naturalist* 138:543–567.
- Wake, D. B. 2012. Facing extinction in real time. *Science* 335:1052–1053.
- Waldron, J. L., and W. J. Humphries. 2005. Arboreal habitat use by the green salamander, *Aneides aeneus*, in South Carolina. *Journal of Herpetology* 39:486–492.
- Wiens, J. 2007. Species delimitation: new approaches for discovering diversity. *Systematic Biology* 56:875–878.
- Wynn, A., and W. R. Heyer. 2001. Do geographically widespread species of tropical amphibians exist? An estimate of genetic relatedness within the neotropical frog *Leptodactylus fuscus* (Schneider 1799) (Anura Leptodactylidae). *Tropical Zoology* 14:255–285.
- Yang, Z. 2015. The BPP program for species tree estimation and species delimitation. *Current Zoology* 61:854–865.
- Yang, Z., and B. Rannala. 2010. Bayesian species delimitation using multilocus sequence data. *Proceedings of the National Academy of Sciences of the United States of America* 107:9264–9269.
- Zhang, J., P. Kapli, P. Pavlidis, and A. Stamatakis. 2013. A general species delimitation method with applications to phylogenetic placements. *Bioinformatics* 29:2869–2876.